iScience, Volume *23*

Supplemental Information

Tuning the Binding Affinity of Heme-Responsive Biosensor for Precise and Dynamic Pathway Regulation

Jian Zhang, Zhiguo Wang, Tianyuan Su, Huanhuan Sun, Yuan Zhu, Qingsheng Qi, and Qian Wang

Supplementary Files

Tuning the binding affinity of heme-responsive biosensor for precise and dynamic pathway regulation

Jian Zhang[1], Zhiguo Wang[2], Tianyuan Su[1], Huanhuan Sun[1], Yuan Zhu[1], Qingsheng Qi[1,3*], Qian Wang[1*]

1. State Key Laboratory of Microbial Technology, National Glycoengineering Research Center, Shandong University, Qingdao 266237, P. R. China
2. Institute of Ageing Research, School of Medicine, Hangzhou Normal University, Hangzhou, 311121, P. R. China
3. CAS Key Lab of Biobased Materials, Qingdao Institute of Bioenergy and Bioprocess Technology, Chinese Academy of Sciences, Qingdao 266101, P. R. China

*Corresponding authors:

Qingsheng Qi

Tel: 0532-58632580, E-mail: qiqingsheng@sdu.edu.cn;

Qian Wang

Tel: 0532-58631580, E-mail: qiqi20011983@gmail.com, lead contact author

TRANSPARENT METHOD

General procedure

All the strains used in this study were summarized in Supplementary Table S3. Molecular cloning and manipulation of plasmids were done with *E. coli* DH5α. All the plasmids and oligonucleotides used in this work were listed in Supplementary Table S4 and Table S5.

Construction of heme biosensor

To construct a related plasmid that characterizes HrtR function, the *hrtR* and *gfp* genes were generated by PCR with primers hrtR-F/hrtR-R, gfp-F/gfp-R, respectively. Chloramphenicol resistance gene and p15A ori were cloned with primers p15A-F/p15A-R using plasmid pACYC184 as the template. Then the three fragments were assembled together using the Gibson method(Gibson et al., 2009) to obtain the plasmid P1. To construct plasmids P0, P2, P3 and P4, the resulting fragments were transformed into *E. coli* DH5α after the treatment by T4 PNK and T4 ligase, which generated by primers p0-F/p0-R, p2-F/p2-R, p3-F/p3-R, p4-F/p3-R were performed, respectively.

Construction and characterization of HrtR saturation mutant library

All HrtR mutants were obtained by using plasmid P1 as template, the primers used for the mutation are listed in Supplementary Table S5. Phanta Max Super-Fidelity DNA Polymerase P505 (Vazyme Biotech Co.,Ltd) was used in all PCR reactions. Resulting fragment was assembled using the Gibson method. The obtained plasmids were transferred into DH5α, respectively, and the obtained strain was cultured in a 24-well plate. After 24 hours of culture, the green fluorescence intensity was detected by a microplate reader. (GFP: exciting light: 485nm, emission light: 528nm).

Construction and optimization of the regulatory system

The strain that regulation *mkate2* contains plasmids PDMGn (n=1, 2, 3, 4, 5) and PSX (X=A,B,O). For pDMG1 construction, chloramphenicol resistance gene and p15A ori were amplified with primers ori-F/ori-R-1. Promoter BBa-J23113 of dcas9 was included in the primer ori-R-1. *dcas9* and *mkate2* gene were cloned with primers dcas9-F/dcas9-R and

mkate-F/mkate-R, degradation tags AAV (AANDENYAAAV) and LAA (AANDENYALAA) are added to the corresponding primers, respectively. Fragments containing different promoters were fused by overlap PCR with primer mkate-F2 and ori-R-1. Resulting fragment was assembled using the Gibson method. Similarly, promoters BBa-J23117, Ba-J23114, Ba-J23110 and Ba-J23100 were contained in primers ori-R-2, ori-R-3, ori-R-4 and ori-R-5, respectively. The construction method of pDMG2, pDMG3, pDMG4 and pDMG5 were the same as above. The construction method of pDMG0 is the same as that of P0, using pDMG4 as a template and primers pair pdmg0-F/pdmg0-R. PDMG4 was cloned as a template using primers M1-F and M1-R, M2-F and M2-R, M2-F and M3-R, resulting fragment were transformed into *E. coli* DH5α after the treatment by T4 PNK and T4 ligase to obtain the plasmid pDMG4-1, pDMG4-2 and pDMG4-3.

For pSA and pSB construction, sgRNA-A and sgRNA-B were cloned with primer pairs sgrna-a-F/sgrna-R, sgrna-b-F/sgrna-R, respectively. *hrtR* was amplified using primer sensor-F and sensor-R. then *hrtR* and Different sgRNAs were assembled using the Gibson method with the plasmid puc19 digested with *Bam*HI. The construction method of pSO is the same as that of P0, using pSIB as a template and psio-F/psio-R as primers.

Plasmids PBHn (n=1, 2, 3) was constructed by adding sgRNA targeting *hemB* to PSB. Different sgRNAs targeting *hemB* were amplified using primers sg-1-F/sg-1-R, sg-2-F/sg-2-R, sg-3-F/sg-3-R, respectively. pSB cloned with primers site-F/site-R was used as the backbone. SgRNA-1, sgRNA-2 and sgRNA-3 were assembled using the Gibson method with the backbone, respectively. At the same time, we replaced the backbone with pSO based on pBH2 to obtain the plasmid pOH2. Remove the *hrtO* from the primer sg-2-F and use it to amplify with sg-1-R, resulting fragment was assembled using the Gibson method with the backbone pSB to obtain the plasmid pOBH2.

The obtained plasmids were transferred into DH5α, respectively, the specific conditions of the plasmid contained in the strain refer to Supplementary Table S3, And the obtained strain was cultured in a 24-well plate and the red fluorescence intensity was detected in real time using a microplate reader (mKATE: exciting light: 590nm, emission light: 645nm).

Construction of ALA, PBG and Porphyrin biosynthesis system

The gene *hemA* from *Salmonella Arizona* and *hemL* from *E. coli* was cloned with primers AL-F/AL-R using pDAL as a template. The plasmid pSB, pSBH2 and pOSBH2 were amplified using primers 10B-gj-F/10B-gj-R, respectively. After digestion with *Xho*I and *Not*I, *hemA-hemL* were cloned into the above linearized plasmids cut with *Xho*I and *Not*I to obtain the plasmid pSBAL, pBH2AL and pOBH2AL. For pBH2ALT construction, *gltW* was cloned with primers tRNA-F/tRNA-R, the backbone was amplified with primers tRNA-gj-F/tRNA-gj-R using pBH2AL as a template. The two fragments were assembled using the Gibson method. The *gdhA* gene in *E. coli* was cloned and integrated into the PCLA plasmid by Gibson method to construct the PCLAG plasmid.

The pCAL and PHAL were cloned with primers CAL-F/CAL-R and HAL-F/HAL-R using pSBAL and as a template, resulting fragment were transformed into *E. coli* DH5α after the treatment by T4 PNK and T4 ligase. pOCAL and POHAL were obtained using the same method, using pCAL and pHAL as a template and CO-F/CO-R and HO-F/ HO-R as primers. The obtained plasmids were transferred into DH5α, respectively, the specific conditions of the plasmid contained in the strain refer to Supplementary Table S3. The medium composition and culture conditions used in the fermentation process were the same as the previous report. ALA and PBG concentration were analyzed using modified Ehrlich's reagent(Kang et al., 2011). Porphyrin compounds were detected by HPLC.

Quantitative real-time PCR (RT-PCR)

The primers studied in this work were listed in Supplementary Table S5. The message RNA (mRNA) level was measured by RT-PCR. The Sample for extracting mRNA were harvested and frozen immediately at -80 ℃. mRNA of hemB and dcas9 was extracted using the RNeasy Mini Kit (Tiangen). The cDNA was obtained from reverse transcription and RT-PCR was carried out in a 96-well plate with a total reaction volume of 20 μL per well in QuantStudioTM3 (Thermo Fisher) using an SYBR® Premix Ex Taq™ II (Perfect Real Time), according to manufacturer's specifications (TaKaRa).

Analysis of heme

The cells were cultured in LB medium, and 1 ml was sampled every 6 hours. The obtained sample was disrupted by Automatic sample grinder (Jingxin, Shanghai), and the supernatant was taken after centrifugation. Intracellular heme concentration was determined using Heme Colorimetric Assay Kit (BioVision, USA).

Dose response curve

Mutants were cultured in LB medium supplemented with 0.05μM, 0.1μM, 0.25μM, 0.5μM, 1μM, 2.5μM, 5μM, 10μM and 20μM heme respectively. Cells were cultured in a 96-well plate and the fluorescence intensity was measured at 8h. GraphPad was used to draw the dose response curve and calculate various parameters.

Heme titration

Purification of HrtR and heme titration experiments referred to the methods of Sawai et al (Sawai et al., 2012).

Molecular dynamics

The molecular dynamics(Mazumder and Case) simulations were performed on the heme bound HrtR/mutant dimers (PDB ID: 3VP5)(Sawai et al., 2012) by using the AMBER 12 software(Case et al., 2005). The FF14SB force field(Maier et al., 2015) was applied for the HrtR proteins. The point charges of heme were calculated with antechamber[4] based on the restricted electrostatic potential (RESP) procedure(Bayly et al., 1993). Bonded terms at the Fe center were calculated according to Seminario's method based on second - derivatives(Seminario, 1996; Villarino et al., 2018), the GAFF force field(Wang et al., 2004) was adopted for the remaining atoms of heme. The binding complexes were individually immersed into the center of a truncated octahedron box of TIP3P water molecules with a margin distance of 10.0 Å, Na^+ counterions were added with the AMBER XLEAP module to keep system in electric neutrality(Case et al., 2005). Each system was firstly energy minimized using the steepest descent method for 5000 steps with the binding complex restricted by a harmonic constraint of 100 kcal·$mol^{-1}Å^{-2}$. A further conjugate gradient minimization of 5000 steps was performed with no constraint. Then the system was gradually heated from 0 K to 300 K under the NVT ensemble over a period of 1 ns, during

which the Langevin thermostat with a coupling coefficient of 1.0 ps and a weak constraint of 10 kcal·mol^{-1}Å^{-2} on the binding complex was applied. Each model was subjected to an equilibrium simulation for 1 ns with no constraint and then a 20 ns production MD simulation under NPT ensemble. Periodic boundary conditions were applied. System temperature was kept 300 K using the Berendsen thermostat with a time constant of 1 ps. Isotropic constant pressure was maintained using Berendsen pressure coupling algorithm with a time constant of 1 ps. Hydrogens involved in covalent bonds were constrained by the SHAKE algorithm(Ryckaert J P 1976). The long-range electrostatic interactions were treated by the Particle Mesh Ewald (PME) method(Essmann et al., 1995). The cutoffs for long-range electrostatic and Van der Waals interactions were both set to 10.0 Å. The time step was set to 2 fs, the coordinates were saved every 1 ps to record the MD trajectory.

Binding free energy

By neglecting the coordinate bonding interactions between HrtR and heme, their intermolecular binding free energy (ΔG_{bind}) was calculated using the molecular mechanics combined with generalized Born and surface area solvation (MM/GBSA) approach(Kollman et al., 2000):

$$\Delta G_{bind} = G_{complex} - (G_{G4} + G_{APC}) \quad (1)$$

$$\Delta G_{bind} = \Delta H - T\Delta S \approx \Delta E_{MM} + \Delta G_{solv} - T\Delta S \quad (2)$$

$$\Delta E_{MM} = \Delta E_{int} + \Delta E_{vdW} + \Delta E_{ele} \quad (3)$$

$$\Delta G_{solv} = \Delta G_{GB} + \Delta G_{SA} \quad (4)$$

Where E_{MM} is the gas phase interaction energy comprising internal strain energy (E_{int}), van der Waals energy (E_{vdW}) and electrostatic energy (E_{ele}). G_{solv} is the solvation free energy comprising contributions form a polar part (G_{GB}) and a nonpolar part (Taverna et al.). ΔE_{int} can be neglected in the current system. ΔG_{GB} was estimated using the generalized Born model with the interior and exterior dielectric constants set to 4 and 80, respectively. ΔG_{SA} was estimated using the LCPO algorithm(Weiser et al., 1999): $\Delta G_{SA} = \gamma\Delta SASA + \beta$, where γ and β were set to 0.0072 and 0, respectively. By performing the normal mode analysis (NMA), $T\Delta S$ that represents the entropy contribution was estimated using the NMODE module. Snapshots were extracted from the last 5 ns trajectories with an interval of 25 ps for the calculations of ΔE_{vdW}, ΔE_{ele}, ΔG_{GB} and ΔG_{SA}. While for the calculation of entropy, only 50 snapshots was evenly extracted from the last 5 ns trajectories due to the expensive computational cost of NMA(Liu et al., 2018).

Supplementary Figures

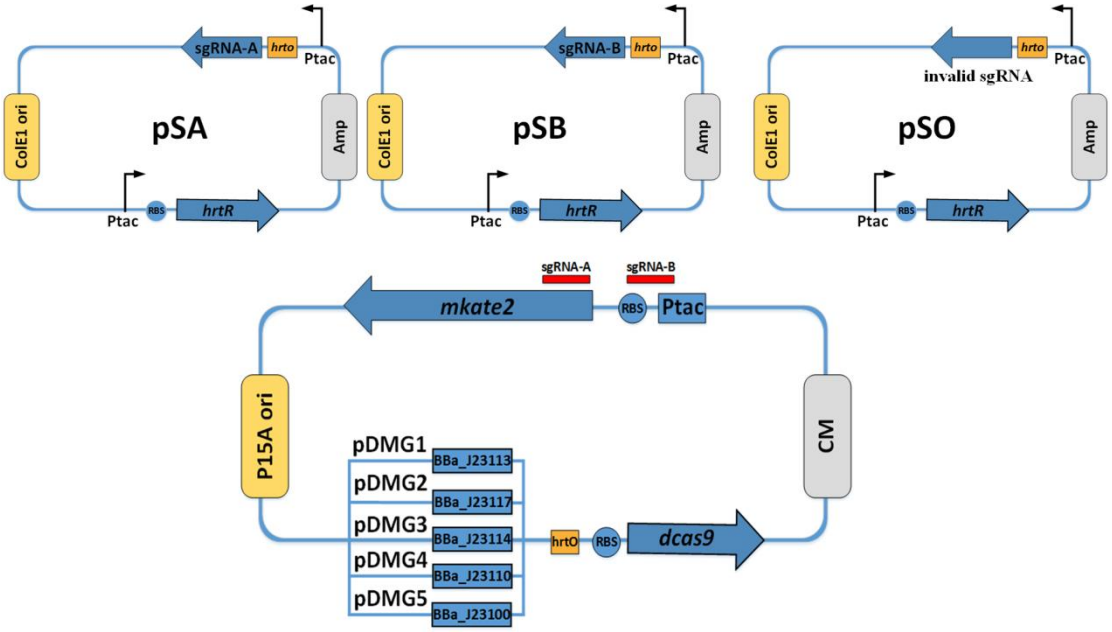

Figure S1: sgRNA-A acts at the 5' end 24bp-44bp of *mkate2*; sgRNA-B acts at the middle of promoter and RBS of *mkate2*; sgRNA-C does not contain a spacer site. Related to Figure 5

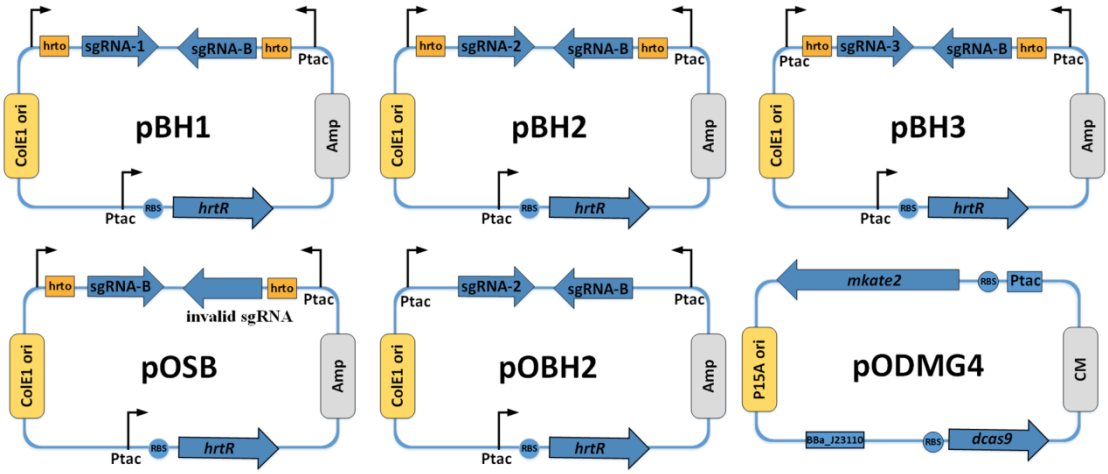

Figure S2: The schematic diagram of plasmids pBHn (n=1,2,3), pOSB, pOBH2, pODMG4. Related to Figure 6

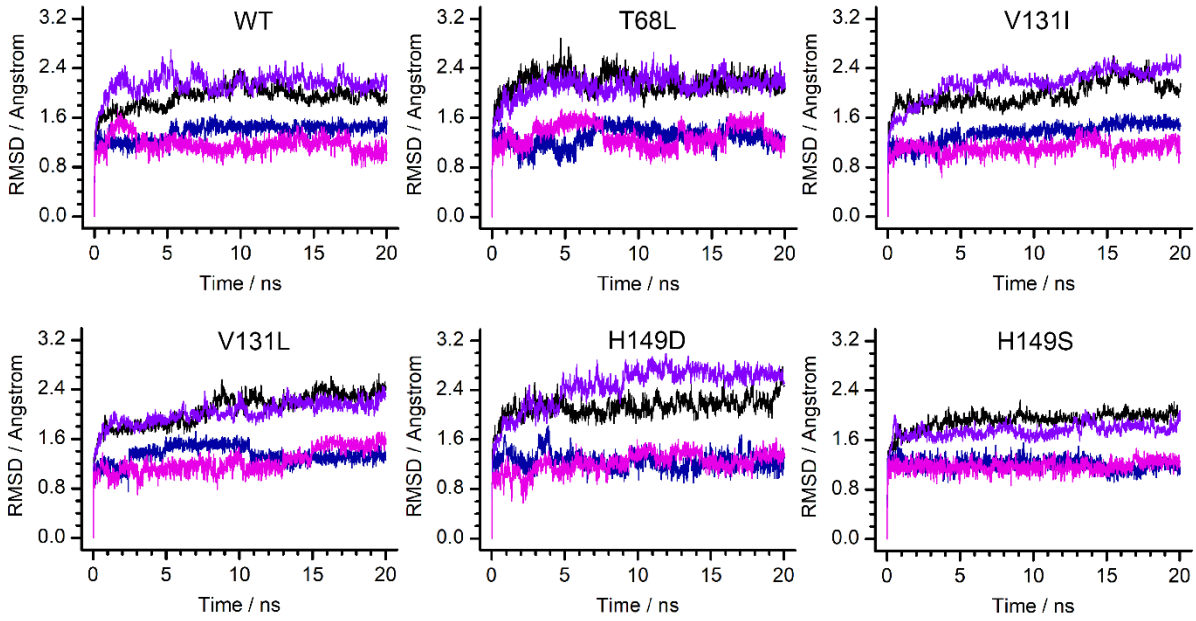

Figure S3,. The root-mean-square deviations (RMSDs) of the HrtR dimer during molecular dynamics. The RMSDs are colored in black and purple for the HrtR proteins in chain A and chain B, respectively. The RMSDs of the heme molecules that bind to the chain A and chain B are colored in navy blue and magenta, respectively. Related to Figure 3

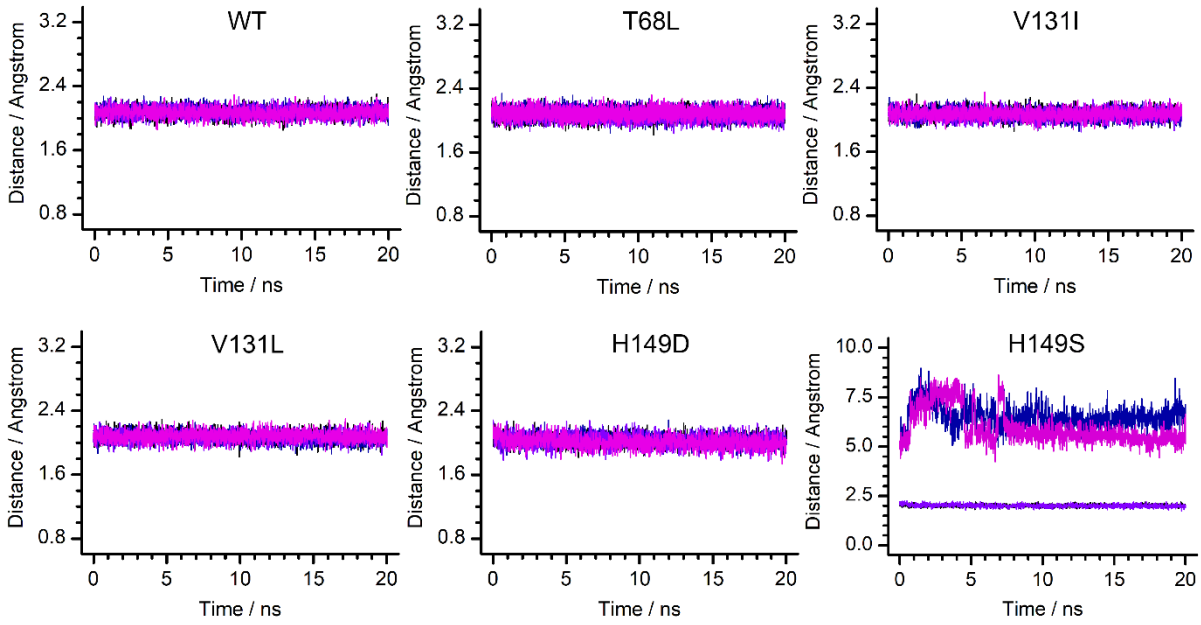

Figure S4. The distances between the heme Fe atom and the HrtR residues. The distance curves between heme Fe atom and NE2 atoms of H72 from chain A and chain B are colored in black and purple, respectively. The distance curves between heme Fe atom and NE2/OD1/OG atoms of H149/D149/S149 from chain A and chain B are colored in navy blue and magenta, respectively. Related to Figure 3

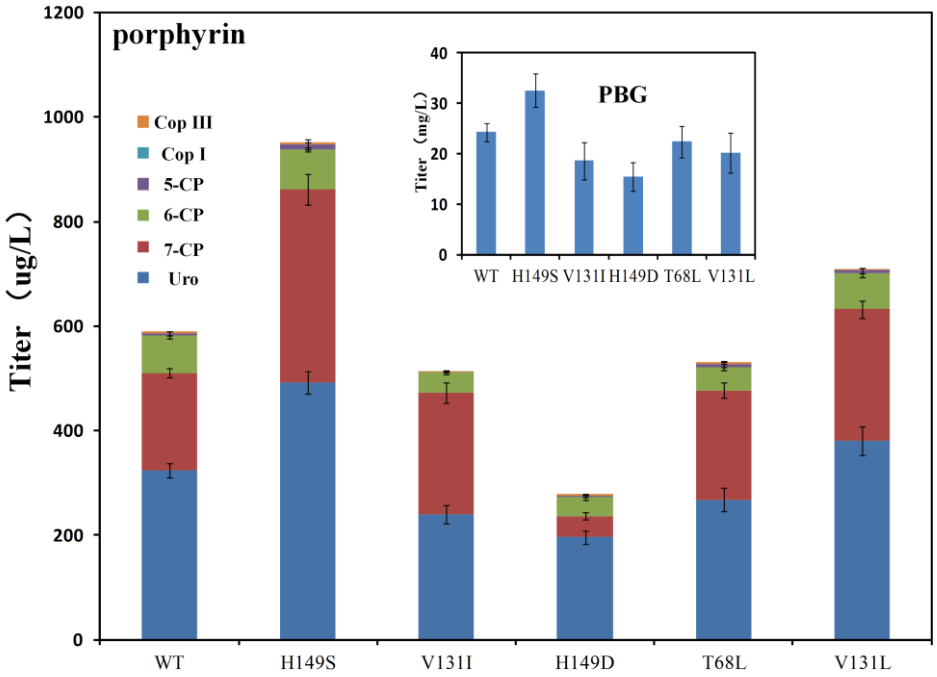

231

232 Figure S5. Accumulation of porphyrins and PBG in different mutant during ALA production;

233 Error bars represent ±1 SD from the mean of three replicate cultures. Related to Figure 7

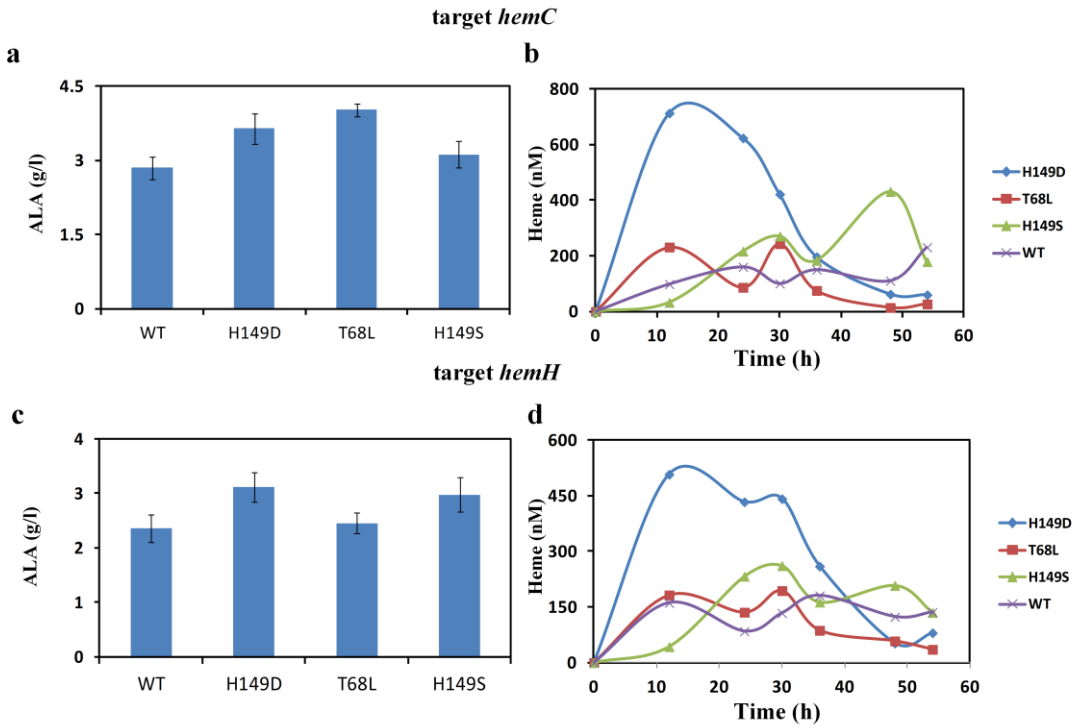

Figure S6. a: Accumulation of ALA in different mutants during PBG production; b: Intracellular free heme concentration curve of the strain target *hemC*; c: Accumulation of ALA in different mutants during porphyrins production; b: Intracellular free heme concentration curve of the strain target *hemH*. Error bars represent ±1 SD from the mean of three replicate cultures. Related to Figure 8

Supplementary Tables

Table S1. Fluorescence intensity of GFP under the control of different mutants. Related to Figure 2

	N	K	T	S	R	I	M	H	Q	P
Thr68	27719	32044	13628	27379	27528	12095	22640	30604	24327	38225
Val131	4518	5690	6159	7516	7545	5576	6671	7692	7153	7427
His149	5081	5930	6374	30161	6607	6347	7628	13628	5281	30290
	L	**D**	**E**	**A**	**G**	**V**	**Y**	**C**	**W**	**F**
Thr68	6937	36889	35757	25694	22389	19316	27781	12065	35333	10994
Val131	14183	5788	5395	9991	5741	13628	9273	6463	10936	11663
His149	6209	4442	4413	6345	6021	7540	7130	7028	7685	6582

Table S2. Binding free energies between HrtR and heme[a]. Related to Figure 3

P450	Energy components[b]						
	ΔE_{ele}	ΔE_{vdW}	ΔG_{GB}	ΔG_{SA}	ΔH	$-T\Delta S$	ΔG_{bind}
WT	190.59	1.69	-155.66	-9.12	27.49	30.09	57.58
T68L	177.64	14.27	-147.91	-8.81	35.19	30.66	65.85
V131I	223.01	6.14	-188.54	-8.89	31.72	34.88	66.60
V131L	138.60	12.36	-111.28	-9.08	30.60	29.25	59.85
H149D	297.42	18.55	-262.79	-8.79	44.39	35.10	79.49
H149S	135.06	-49.53	-118.95	-9.37	-42.78	32.90	-9.88

[a] The binding free energies were calculated by neglecting the coordinate bonding interactions between HrtR and heme since the molecular dynamics method is unproper to compute the intermolecular binding affinity with covalent bond involved. Therefore, the values of ΔG_{bind} presented here represent the binding susceptibility of heme to the HrtR variants instead of absolute binding free energies.

[b] Energies are in kcal·mol^{-1}.

Table S3. Bacterial strains used in this study. Related to Figure 1,2,3,5,6,7 and 8.

Strains	Relevant properties	Source
DH5α		**lab stock**
S1	**MG1655 integrates a copies of *hemA*/*hemL* on the genome**	**lab stock**
S20	**MG1655 integrates 20 copies of *hemA*/*hemL* on the genome**	**lab stock**
S35	**MG1655 integrates 35 copies of *hemA*/*hemL* on the genome**	**lab stock**
S65	**MG1655 integrates 65 copies of *hemA*/*hemL* on the genome**	**lab stock**
S100	**MG1655 integrates 100 copies of *hemA*/*hemL* on the genome**	**lab stock**
S1P1	**S1 harboring P1**	**this study**
S20P1	**S20 harboring P1**	**this study**
S35P1	**S35 harboring P1**	**this study**
S65P1	**S65 harboring P1**	**this study**
S100P1	**S100 harboring P1**	**this study**
SP0	**DH5α harboring P0**	**this study**
SP1	**DH5α harboring P2**	**this study**
SP2	**DH5α harboring P3**	**this study**
SP3	**DH5α harboring P4**	**this study**
SP4	**DH5α harboring P5**	**this study**
SP1-T68L	**DH5α harboring P1-T68L**	**this study**
SP1-V131L	**DH5α harboring P1-V131L**	**this study**
SP1-V131I	**DH5α harboring P1-V131I**	**this study**
SP1-H149D	**DH5α harboring P1-H149D**	**this study**
SP1-H149S	**DH5α harboring P1-H149S**	**this study**
SO1	**DH5α harboring PSO+PDMG1**	**this study**
SO2	**DH5α harboring PSO+PDMG2**	**this study**
SO3	**DH5α harboring PSO+PDMG3**	**this study**
SO4	**DH5α harboring PSO+PDMG4**	**this study**
SO5	**DH5α harboring PSO+PDMG5**	**this study**
SA1	**DH5α harboring PSA+PDMG1**	**this study**
SA2	**DH5α harboring PSA+PDMG2**	**this study**
SA3	**DH5α harboring PSA+PDMG3**	**this study**
SA4	**DH5α harboring PSA+PDMG4**	**this study**
SA5	**DH5α harboring PSA+PDMG5**	**this study**
SB1	**DH5α harboring PSB+PDMG1**	**this study**
SB2	**DH5α harboring PSB+PDMG2**	**this study**
SB3	**DH5α harboring PSB+PDMG3**	**this study**
SB4	**DH5α harboring PSB+PDMG4**	**this study**
SB5	**DH5α harboring PSB+PDMG5**	**this study**
SH0	**DH5α harboring PDMG4+POSB**	**this study**
SH1	**DH5α harboring PDMG4+PBH1**	**this study**
SH2	**DH5α harboring PDMG4+PBH2**	**this study**
SH3	**DH5α harboring PDMG4+PBH3**	**this study**
SOH	**DH5α harboring PODMG4+POBH2**	**this study**
SH2-AL-1	**DH5α harboring PBH2-AL+PDMG4-1**	**this study**
SH2-AL-2	**DH5α harboring PBH2-AL+PDMG4-2**	**this study**
SH2-AL-3	**DH5α harboring PBH2-AL+PDMG4-3**	**this study**
SOH-AL	**DH5α harboring PODMG4+POBH2-AL**	**this study**
SB4-AL	**DH5α harboring PSB-AL+PDMG4**	**this study**

SH2-AL	**DH5α harboring PDMG4+PBH2-AL**	**this study**
SH2-ALT	**DH5α harboring PDMG4+PBH2ALT**	**this study**
SH2-ALTG	**DH5α harboring PDMG4+PBH2ALTG**	**this study**
ST-T68L	**DH5α harboring PDMG4+PBH2ALTG-T68L**	**this study**
ST-V131L	**DH5α harboring PDMG4+PBH2ALTG-V131L**	**this study**
ST-V131I	**DH5α harboring PDMG4+PBH2ALTG-V131I**	**this study**
ST-H149D	**DH5α harboring PDMG4+PBH2ALTG-H149D**	**this study**
ST-H149S	**DH5α harboring PDMG4+PBH2ALTG-H149S**	**this study**
SAL-C	**DH5α harboring PDMG4+PCAL**	**this study**
SAL-CO	**DH5α harboring PODMG4+POCAL**	**this study**
SAL-C-H149D	**DH5α harboring PDMG4+PCAL-H149D**	**this study**
SAL-C-H149S	**DH5α harboring PDMG4+PCAL-H149S**	**this study**
SAL-C-T68L	**DH5α harboring PDMG4+PCAL-T68L**	**this study**
SAL-H	**DH5α harboring PDMG4+PHAL**	**this study**
SAL-HO	**DH5α harboring PODMG4+POHAL**	**this study**
SAL-H-H149D	**DH5α harboring PDMG4+PHAL-H149D**	**this study**
SAL-H-H149S	**DH5α harboring PDMG4+PHAL-H149S**	**this study**
SAL-H-T68L	**DH5α harboring PDMG4+PHAL-T68L**	**this study**

311 Table S4. Plasmids used in this study. Related to Figure 1,2,3,5,6,7 and 8.

Plasmids	Charecteristics	Source
P0	**pACYC184 contains gfp and HrtR**	**this study**
P1	**pACYC184 contains HrtO, gfp and HrtR**	**this study**
P1-T68L	**pACYC184 contains gfp and HrtR-T68L**	**this study**
P1-V131L	**pACYC184 contains gfp and HrtR-V131L**	**this study**
P1-V131I	**pACYC184 contains gfp and HrtR-V131I**	**this study**
P1-H149D	**pACYC184 contains gfp and HrtR-H149D**	**this study**
P1-H149S	**pACYC184 contains gfp and HrtR-H149S**	**this study**
PSO	**pUC19 contains HrtR and HrtO-ineffective sgRNA**	**this study**
PSA	**pUC19 contains HrtR and HrtO-sgRNA-A**	**this study**
PSB	**pUC19 contains HrtR and HrtO-sgRNA-B**	**this study**
POSB	**pUC19 contains HrtR and sgRNA-B**	**this study**
PDMG1	**pACYC184 contains mkate2 and dcas9 (promoter:$_{J23113}$)**	**this study**
PDMG2	**pACYC184 contains mkate2 and dcas9 (promoter:$_{J23117}$)**	**this study**
PDMG3	**pACYC184 contains mkate2 and dcas9 (promoter:$_{J23114}$)**	**this study**
PDMG4	**pACYC184 contains mkate2 and dcas9 (promoter:$_{J23110}$)**	**this study**
PDMG5	**pACYC184 contains mkate2 and dcas9 (promoter:$_{J23100}$)**	**this study**
PODMG4	**PDMG4 deletes HrtO**	**this study**
PBH1	**pSIB contains sgRNA-1**	**this study**
PBH2	**pSIB contains sgRNA-2**	**this study**
PBH3	**pSIB contains sgRNA-3**	**this study**
POBH2	**pSIBH2 with the deletion of HrtO**	**this study**
PDMG4-1	**The promoter of mkate2 in PDMG4 was replaced with J23110**	**this study**
PDMG4-2	**The promoter of mkate2 in PDMG4 was replaced with J23101**	**this study**
PDMG4-3	**The promoter of mkate2 in PDMG4 was replaced with J23106**	**this study**
POBH2-AL	**POBH2 added *hemA*/*hemL***	**this study**
PSB-AL	**PSB added *hemA*/*hemL***	**this study**
PBH2-AL	**PBH2 added *hemA*/*hemL***	**this study**
PBH2ALT	**PBH2AL added tRNA-GLU**	**this study**
PBH2ALTG	**PBH2ALT added *rhtA* and *gdhA***	**this study**
PBH2ALTG-T68L	**PBH2ALTG with HrtR-T68L**	**this study**
PBH2ALTG-V131L	**PBH2ALTG with HrtR-V131L**	**this study**
PBH2ALTG-V131I	**PBH2ALTG with HrtR-V131I**	**this study**
PBH2ALTG-H149D	**PBH2ALTG with HrtR-H149D**	**this study**
PBH2ALTG-H149S	**PBH2ALTG with HrtR-H149S**	**this study**
PCAL	**replace with sgRNA targeting *hemC* on the basis of PBH2ALT**	**this study**
POCAL	**PCAL with the deletion of HrtO**	**this study**
PCAL-H149D	**PCAL with HrtR-H149D**	**this study**
PCAL-H149S	**PCAL with HrtR-H149S**	**this study**
PCAL-T68L	**PCAL with HrtR-T68L**	**this study**
PHAL	**replace with sgRNA targeting *hemH* on the basis of PBH2ALT**	**this study**
POHAL	**PHAL with the deletion of HrtO**	**this study**

PHAL-H149D	**PHAL with HrtR-H149D**	**this study**
PHAL-H149S	**PHAL with HrtR-H149S**	**this study**
PHAL-T68L	**PHAL with HrtR-T68L**	**this study**
PCHUA	**pcolAduet1 contains *chuA***	**this study**
p15b-WT	**p15b contains HrtR-WT**	**this study**
p15b-H149D	**p15b contains HrtR-H149D**	**this study**
p15b-H149S	**p15b contains HrtR-H149S**	**this study**
p15b-T68L	**p15b contains HrtR-T68L**	**this study**
p15b-V131L	**p15b contains HrtR-V131L**	**this study**
p15b-V131I	**p15b contains HrtR-V131I**	**this study**

References

Bayly, C.I., Cieplak, P., Cornell, W.D., and Kollman, P.A. (1993). A Well-Behaved Electrostatic Potential Based Method Using Charge Restraints for Deriving Atomic Charges - the Resp Model. J Phys Chem-Us *97*, 10269-10280.

Case, D.A., Cheatham, T.E., Darden, T., Gohlke, H., Luo, R., Merz, K.M., Onufriev, A., Simmerling, C., Wang, B., and Woods, R.J. (2005). The Amber biomolecular simulation programs. J Comput Chem *26*, 1668-1688.

Essmann, U., Perera, L., Berkowitz, M.L., Darden, T., Lee, H., and Pedersen, L.G. (1995). A Smooth Particle Mesh Ewald Method. J Chem Phys *103*, 8577-8593.

Gibson, D.G., Young, L., Chuang, R.Y., Venter, J.C., Hutchison, C.A., and Smith, H.O. (2009). Enzymatic assembly of DNA molecules up to several hundred kilobases. Nat Methods *6*, 343-U341.

Kang, Z., Wang, Y., Gu, P.F., Wang, Q., and Qi, Q.S. (2011). Engineering Escherichia coli for efficient production of 5-aminolevulinic acid from glucose. Metab Eng *13*, 492-498.

Kollman, P.A., Massova, I., Reyes, C., Kuhn, B., Huo, S.H., Chong, L., Lee, M., Lee, T., Duan, Y., Wang, W.*, et al.* (2000). Calculating structures and free energies of complex molecules: Combining molecular mechanics and continuum models. Accounts of chemical research *33*, 889-897.

Liu, N., Zhou, W.F., Guo, Y., Wang, J.M., Fu, W.T., Sun, H.Y., Liu, D., Duan, M.J., and Hou, T.J. (2018). Molecular Dynamics Simulations Revealed the Regulation of Ligands to the Interactions between Androgen Receptor and Its Coactivator. J Chem Inf Model *58*, 1652-1661.

Maier, J.A., Martinez, C., Kasavajhala, K., Wickstrom, L., Hauser, K.E., and Simmerling, C. (2015). ff14SB: Improving the Accuracy of Protein Side Chain and Backbone Parameters from ff99SB. Journal of chemical theory and computation *11*, 3696-3713.

Mazumder, D., and Case, D.A. (2007). AMBER Score in DOCK6: Application of molecular dynamics simulations and implicit solvent model (GB/SA) in protein-ligand docking. Abstr Pap Am Chem S *233*, 20-20.

Ryckaert J P , C.G., Berendsen H J C . (1976). Numerical integration of the cartesian equations of motion of a system with constraints: molecular dynamics of n-alkanes[J]. Journal of Computational Physics, 327-341.

Sawai, H., Yamanaka, M., Sugimoto, H., Shiro, Y., and Aono, S. (2012). Structural Basis for the Transcriptional Regulation of Heme Homeostasis in Lactococcus lactis. J Biol Chem *287*, 30755-30768.

Seminario, J.M. (1996). Calculation of intramolecular force fields from second-derivative tensors. Int J Quantum Chem *60*, 1271-1277.

Taverna, P., Rendahl, K., Jekic-McMullen, D., Shao, Y., Aardalen, K., Salangsang, F., Doyle, L., Moler, E., and Hibner, B. (2007). Tezacitabine enhances the DNA-directed effects of fluoropyrimidines in human colon cancer cells and tumor xenografts. Biochem Pharmacol *73*, 44-55.

Villarino, L., Splan, K.E., Reddem, E., Alonso-Cotchico, L., de Souza, C.G., Lledos, A., Marechal, J.D., Thunnissen, A.M.W.H., and Roelfes, G. (2018). An Artificial Heme Enzyme for Cyclopropanation Reactions. Angew Chem Int Edit *57*, 7785-7789.

Wang, J.M., Wolf, R.M., Caldwell, J.W., Kollman, P.A., and Case, D.A. (2004). Development and testing of a general amber force field. J Comput Chem *25*, 1157-1174.

383 Weiser, J., Shenkin, P.S., and Still, W.C. (1999). Approximate solvent-accessible
384 surface areas from tetrahedrally directed neighbor densities. Biopolymers *50*, 373-
385 380.

386